Catalysis Today 157 (2010) 451–455

Contents lists available at ScienceDirect

Catalysis Today

journal homepage: www.elsevier.com/locate/cattod

$Ir/Ce_{0.9}Gd_{0.1}O_{2-x}$ as a new potential anode component in solid oxide fuel cells integrating the concept of gradual internal reforming of methane

J. Toyir [1], P. Gélin *, H. Belatel, A. Kaddouri

Université Lyon 1, CNRS, UMR 5256, IRCELYON, Institut de recherches sur la catalyse et l'environnement de Lyon, 2 avenue Albert Einstein, F-69626 Villeurbanne, France

ARTICLE INFO

Keywords:
Steam reforming of methane
Iridium
Gd-doped ceria
Synergetic effect

ABSTRACT

$Ce_{0.9}Gd_{0.1}O_{2-x}$-supported iridium catalyst containing 0.1 wt% Ir was prepared and studied in the steam reforming of methane under water deficient conditions ($H_2O/CH_4 = 0.1$) in order to evaluate its potential use as anode material in solid oxide fuel cells directly fed with methane and integrating a gradual internal reforming (GIR) concept. Catalytic activity of $Ce_{0.9}Gd_{0.1}O_{2-x}$ (CGO) and Ir/Al_2O_3 (0.1 wt% Ir) was also measured. Attention was paid to carbon deposition. Catalysts were characterized by temperature programmed reaction experiments in dry methane (TPR-CH_4) followed by mass spectrometry. Adding Ir to CGO was shown to result in a catalyst much more active than CGO and Ir/Al_2O_3, being stable and extremely resistant to carbon deposition. Different mechanisms and/or rate determining steps are proposed and discussed to explain the observed different catalytic behaviours depending on the catalyst.

1. Introduction

Solid oxide fuel cells (SOFCs) are promising candidates for stationary power generation which offer the unique advantage to allow internal reforming because they operate at high temperatures with direct use of hydrocarbon fuel to generate energy. This makes it possible to simplify the overall system by taking out the reformer unit and this allows increasing the yield of the cell. This technology emerges as very promising in large and intermediate power generation application. However, this operating mode may result in either carbon deposition at high temperatures or poor power output at low operating temperatures [1,2]. Natural gas as well as biogas (which contains CO_2 and H_2O in addition to CH_4 as the main component) can be used as fuels. The production of biogas from renewable energy sources such as organic wastes or biomass is a serious option for the mitigation of greenhouse gases and therefore global warming control.

Internal reforming of methane is generally achieved using conventional Ni cermets which are very active both in steam reforming of methane and electrochemical oxidation of hydrogen. However, they must be operated at steam to fuel ratios higher than unity (typically 1.5–2) to prevent carbon deposition at the anode inlet [3–8]. This operating mode decreases the overall yield of the cell. It also induces mechanical constraints due to large temperature gradients along the anode. The steam reforming reaction, which is strongly endothermic, occurs mainly at the inlet, producing hydrogen, while electrochemical reactions occur along the anode with heat production. An alternative concept, so called gradual internal reforming (GIR) [9], was proposed to overcome this problem. Accordingly, only very little amount of water is admitted into the cell, thus limiting CH_4 conversion into H_2 at the anode inlet. The progressive conversion of CH_4 is made possible along the anode due to the formation of H_2O resulting from the electrochemical oxidation of H_2. Endothermic and exothermic reactions are then coupled, being delocalized along the anode. Thermal constraints should be then limited and the lifetime of the cell much improved. This requires however the use of alternative materials to Ni-based ones, being moderately active in steam reforming and highly resistant to carbon formation under highly water deficient conditions.

Ceria-containing anodes have been developed for direct methane fuel cell [10,11]. Ceria-doped catalysts have been also reported to exhibit high resistance against carbon deposition during dry or steam reforming of methane [12,13] and it was suggested that this is due to the high ion mobility of ceria-based systems [14]. But their catalytic activity in steam reforming is too low to allow GIR operation at moderate temperatures, typically 800 °C [15]. Recently we have shown that the catalytic activity of gadolinium-doped ceria (CGO) in dry reforming of methane could be strongly improved by adding only small amounts of iridium to the support. The resulting Ir/CGO catalyst exhibited significant and stable catalytic activity at temperatures below 800 °C with no graphitic carbon deposi-

---

* Corresponding author.
E-mail address: patrick.gelin@ircelyon.univ-lyon1.fr (P. Gélin).

[1] On leave from: Université Sidi Mohamed Ben Abdellah Fès, FP-Taza, Equipe de procédés pour l'énergie et l'environnement, BP 1223 Taza, Morocco.

0920-5861/$ – see front matter © 2010 Elsevier B.V. All rights reserved.
doi:10.1016/j.cattod.2010.03.066

tion in conditions thermodynamically favourable to its extensive formation [12].

In the present work Ir/CGO containing 0.1 wt% Ir was prepared and studied in CH_4 steam reforming under strongly water deficient conditions. For comparison, the CGO support and Ir/Al_2O_3 (0.1 wt% Ir) used as a reference catalyst were also studied. Catalysts were characterized by CH_4 temperature programmed reaction experiments. We demonstrate the existence of a synergetic effect between iridium and CGO leading to improved catalytic activity and resistance against carbon deposits formation.

2. Experimental

Ir/CGO and Ir/Al_2O_3 catalysts (0.1 wt% Ir) were prepared by impregnation of $Ce_{0.9}Gd_{0.1}O_{2-x}$ (Praxair, 43 m^2/g) and Al_2O_3 (Rhodia, 110 m^2/g) respectively with iridium acetylacetonate (Aldrich) solutions. Catalytic activity experiments were carried out in a continuous flow system at atmospheric pressure. Blank experiments (without catalyst sample) were performed before each catalytic test, showing no H_2, CO or CO_2 formation. Samples of 200 mg for CGO, 20 mg for Ir/CGO and Ir/Al_2O_3 were introduced into a U-shaped quartz reactor. A thermocouple in contact with the external wall of the reactor at the position where the catalyst bed was located allowed monitoring the catalyst temperature. The samples were pretreated in N_2 (6.5 $L\,h^{-1}$) at 900 °C for 2 h before catalytic testing. The catalytic activity was investigated at molar H_2O/CH_4 ratio: 0.1 using a reactant mixture of 50 mol% CH_4 and 5 mol% H_2O with a total flow rate of 6.5 $L\,h^{-1}$. N_2 was used as the carrier gas. Suitable H_2O concentration was obtained by flowing the adequate mixture of CH_4 and N_2 dry gases throughout a saturator containing distilled water maintained at 33 °C (thermostated bath). Water content at the reactor outlet was determined using a Edgetech Dew Prime I dew point monitor. An M&C ECP gas cooler maintained at 3 °C was used to reduce steam concentration in the feed in order to allow a reliable analysis by gas chromatography. CH_4, H_2, CO and CO_2 were analyzed with a Varian micro-GC equipped with appropriate columns (molecular sieve 5A and Porapak) and thermal conductivity detector (TCD).

Temperature programmed CH_4 reduction (TPR-CH_4) experiments were performed using a Pfeiffer Omnistar quadrupole mass spectrometer. Prior to the experiment, the samples (20 mg) were treated in He up to 900 °C (linear rate of 10 °C/min – 2 h at 900 °C) and then cooled down to room temperature. TPR-CH_4 experiment was carried out in a CH_4 (4900 ppm)/Ar (528 ppm)/He mixture (flow rate of 1.8 $L\,h^{-1}$) at a linear heating rate of 10 °C/min up to 900 °C. The QMS signals for H_2 ($m/e=2$), CH_4 ($m/e=15$), CO ($m/e=28$), CO_2 ($m/e=44$), O_2 ($m/e=32$), H_2O ($m/e=18$) and Ar ($m/e=40$) were continuously monitored as a function of temperature.

3. Results

3.1. Catalytic activity

For all samples catalytic measurements were performed at 750 °C in the presence of a large excess of methane with respect to water vapor. It should be noted that impregnation by iridium did not lead to any significant change in surface area of initial support. The maximum H_2 formation (8.5 vol% H_2) corresponding to about 60% conversion of the limiting reactant was obtained over the Ir/CGO sample. For the other two samples, H_2 concentrations were very small. Depending on the sample, CO, CO_2 or a mixture of two formed with H_2. CO_2 was the only other product observed upon reaction over CGO, while, over Ir/CGO, CO_2 formed in a much lower amount, CO and H_2 being the main products of the reaction. In the case of Ir/Al_2O_3, both CO and CO_2 were observed but CO formed preferentially to CO_2. In addition, while CGO-based catalysts exhibited a constant H_2 production with time on stream, a slight deactivation of the Ir/Al_2O_3 was observed. Table 1 summarizes the steady state rates of formation of H_2, CO and CO_2 measured at 750 °C after 2 and 22 h reaction for CGO, Ir/CGO and Ir/Al_2O_3 samples. It must be kept in mind that the rates measured over Ir/CGO might be possibly influenced by high water conversion levels. Comparison of catalytic activity data of CGO and Ir/CGO clearly demonstrates that Ir addition to CGO has an impressive beneficial effect on the catalytic activity, increasing the H_2 formation rate by more than two orders of magnitude compared to CGO alone. Surprisingly, the catalytic activity of Ir/Al_2O_3 was shown to be low, being only slightly higher than for CGO. This clearly evidences the existence of a synergetic effect between Ir and CGO. The eventual formation of carbon deposits during catalytic testing was evaluated by performing temperature programmed oxidation (TPO) experiments after testing. It was thus confirmed that no carbon deposits were formed over CGO. Only a slight amount of highly reactive C deposited over Ir/CGO, remaining unchanged with time on stream. As a result, no change in catalytic activity was observed between 2 and 22 h. On the contrary, Ir/Al_2O_3 was shown to deactivate progressively with time on stream (Table 1) and the formation of weakly reactive carbon deposits was evidenced after reaction. These species are thought to be responsible for the deactivating behaviour of this sample.

Table 1
Steady state[a] activity after 2 and 22 h in methane steam reforming of CGO, Ir/CGO and Ir/Al_2O_3 catalysts.

Catalysts	Formation rates ($\mu mol\,g^{-1}\,s^{-1}$)			CH_4 consumption rate (moles g^{-1} of metal s^{-1})	$H_2/(3CO+4CO_2)$ ratio
	H_2	CO	CO_2		
CGO					
2 h	2.7	–	0.7	0.007	0.98
22 h	2.7	–	0.7		
Ir/CGO					
2 h	322	81.4	16.6	1.0	1.00
22 h	326	80.0	16.2		
Ir/Al_2O_3					
2 h	11.0	2.4	0.4	0.03	1.25
22 h	6.0	0	0		
7 wt% Ni/MgO[b]				24	

[a] Experimental conditions: 750 °C; 5 vol% H_2O, 50 vol% CH_4, N_2 balance; total flow rate = 6.5 $L\,h^{-1}$; 20 mg Ir/CGO or Ir/Al_2O_3, 200 mg CGO.

[b] From Wei and Iglesia [17]: 700 °C; 33.3 kPa CH_4; 33.3 kPa H_2O; 10 mg Ni/MgO-A; 2 h.

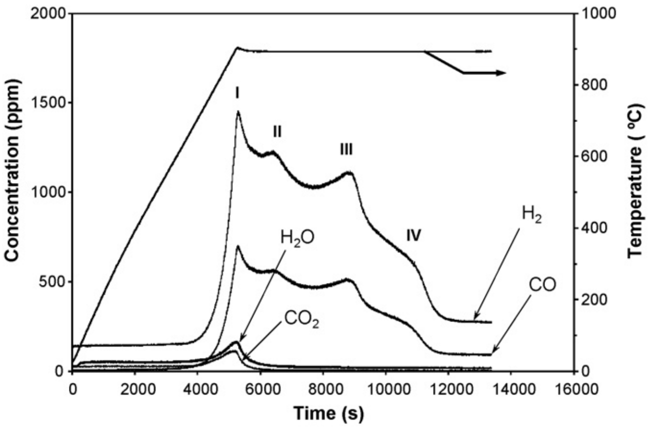

Fig. 1. Gas profiles for CH_4-TPR of CGO. Gas composition: CH_4 (4900 ppm), Ar (528 ppm), He balance; catalyst weight = 22.8 mg; heating rate = 10 °C/min; flow rate = 1.8 L h^{-1}.

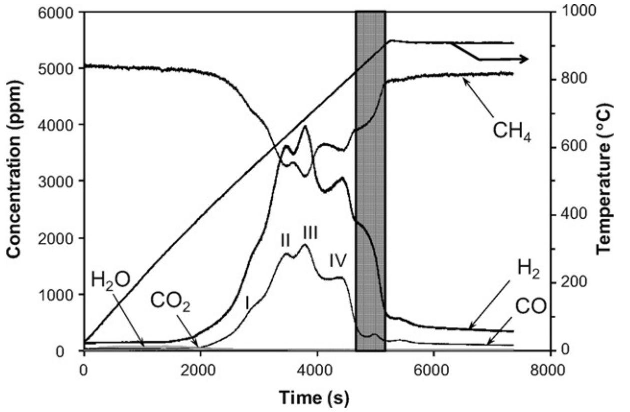

Fig. 2. Gas profiles for CH_4-TPR of Ir/CGO. Gas composition: CH_4 (4900 ppm), Ar (528 ppm), He balance; catalyst weight = 22.8 mg; heating rate = 10 °C/min; flow rate = 1.8 L h^{-1}. Shadow area indicates that carbon deposits form: H_2 is produced from CH_4 without CO formation.

3.2. TPR-CH_4 study

TPR-CH_4 experiments were performed for the three samples in order to more deeply understand the reaction step involving the methane as a reactant in the overall mechanism of CH_4/H_2O reaction(s).

Figs. 1–3 display the H_2, CO, CO_2 and H_2O concentrations as a function of time and temperature during CH_4-TPR of CGO, Ir/CGO and Ir/Al_2O_3 respectively. CH_4 started to react with CGO at ca. 600 °C, producing increasing amounts of H_2, CO, CO_2 and H_2O up to 900 °C. After reaching a temperature plateau at 900 °C, CO_2 and H_2O formations progressively decreased with time while CO and H_2 were still produced, exhibiting three different maximums with time. The observed sharpness of peak 1 is likely due to reaching the temperature plateau but this does not exclude the presence of a maximum at this stage. The formation of CO and CO_2 indicates that methane can reduce Ce^{4+} sites of ceria into Ce^{3+}, the rate of reduction varying upon the extent of ceria reduction. Interestingly, CO and H_2, whenever formed as the only products, were produced in a constant ratio of about 2 until completion of the Ce^{4+} sites reduction. This is consistent with the absence of methane cracking which would lead to H_2 production and carbon deposits formation.

For Ir/CGO catalyst methane started to be converted at ca. 300 °C, which produced H_2 and CO mainly. Some CO_2 and H_2O were also produced. The formation of CO can be attributed again to the reduction of reducible sites of ceria. The temperature at which the process starts turns out to be much lower than for CGO. Four main peaks of H_2 (resp. CO) formation can be identified at ca. 540, 640, 690 and 790 °C in the same way as for CGO, which indicates that Ir/CGO sample is reduced by methane following the same sequence than CGO alone. Between 290 and 745 °C a perfect fit between produced CO and consumed CH_4 profiles was observed, indicating that no carbon deposition arising from methane cracking occurred in this temperature range. Above 745 °C it can be noticed that CH_4 was still consumed with the only production of H_2. The absence of CO formation suggests the completion of the Ce^{4+}/Ce^{3+} reduction process. The formation of H_2 suggests that only methane cracking reaction can proceed at this stage, leading to carbon accumulation on the catalyst. It is worth mentioning that the reaction stops after a while, which indicates that only a limited amount of carbon deposits can form. This confirms the high resistance of Ir/CGO against carbon deposit formation in CH_4/H_2O mixtures with large CH_4 excess. This experiment confirms also the crucial beneficial role of Ir in the reactivity of CGO towards methane.

For Ir/Al_2O_3, very different profiles were obtained compared to CGO-based catalysts (Fig. 3). Only water was detected at the beginning of treatment as a result of desorption of physisorbed water and partial dehydroxylation of the alumina surface. CO formation started along with H_2 release at a temperature of ca. 300–350 °C. This suggests that surface OH groups of the alumina participate to the reaction according to the following global equation:

$$CH_4 + 2OH_s \rightarrow CO + 3H_2 + O_s \tag{1}$$

Two maximums can be clearly distinguished at ca. 460 and 720 °C, tentatively attributed to two distinct hydroxyl types with different reactivities at the Al_2O_3 surface. This overall reaction does not exclude the possible intermediate formation of carbon by methane cracking at Ir metal sites.

During this step, the H_2 to CO ratio was close to 3, suggesting that carbon did not accumulate on the catalyst and the overall reaction (1) proceeded. Above 800 °C the H_2 production rose drastically, suggesting no more reaction of Al_2O_3 hydroxyl groups with methane likely due to their full consumption and only methane cracking to proceed. On the contrary to Ir/CGO, it can be noticed that H_2 production and the C deposition did not stop, continuing to proceed with increasing rate at 900 °C. This confirms that Ir/Al_2O_3 is much less resistant to C formation in GIR conditions.

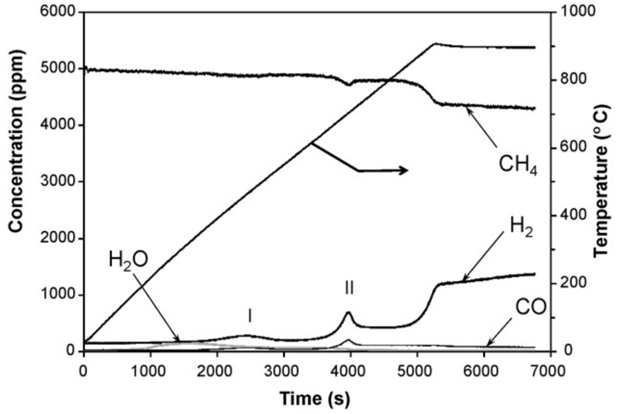

Fig. 3. Gas profiles for CH_4-TPR of Ir/Al_2O_3. Gas composition: CH_4 (4900 ppm), Ar (528 ppm), He balance; catalyst weight = 22.8 mg; heating rate = 10 °C/min; flow rate = 1.8 L h^{-1}.

4. Discussion

At 750 °C in a CH_4/H_2O mixture, the following equilibriums are all possible according to thermodynamics:

$$CH_4 + H_2O \rightleftarrows CO + 3H_2 \quad = \text{steam reforming} \tag{2}$$

$$CO + H_2O \rightleftarrows CO_2 + H_2 \quad = \text{water gas shift} \tag{3}$$

$$CH_4 + 2H_2O \rightleftarrows CO_2 + 4H_2 \quad = \text{reverse methanation} \tag{4}$$

$$CH_4 + CO_2 \rightleftarrows 2CO + 2H_2 \quad = \text{dry reforming} \tag{5}$$

$$CH_4 \rightleftarrows C + 2H_2 \quad = \text{methane cracking} \tag{6}$$

$$C + CO_2 \rightleftarrows 2CO \quad = \text{reverse Boudouard reaction} \tag{7}$$

$$C + H_2O \rightleftarrows CO + H_2 \tag{8}$$

The strongly water deficient conditions used for catalytic testing are thermodynamically favourable to carbon formation at 750 °C. However, it must be derived from our experimental data that carbon deposits did not form over CGO. Only H_2 and CO_2 formed. Similar results were obtained over CGO used by Ramirez-Cabrera et al. [15,16] for catalytic steam reforming under steam to methane ratios as low as 0.6. Only global reaction (4) can be considered to take place on the CGO support alone.

The addition of a small amount of Ir (0.1 wt%) to CGO leads to the formation of H_2 and CO as main products while very few carbon deposits formed (as evidenced by TPO after testing) and did not increase with time on stream. H_2 and CO might form essentially through steam reforming reaction (2) while the formation of small amounts of CO_2 might result from reverse methanation (reaction (4)) or WGS reaction (reaction (3)). Comparing CGO and Ir/CGO, it can be concluded that Ir, even in a very small amount, plays an important role both in catalytic conversion of CH_4/H_2O, which is considerably improved, and in the reactions occurring at the catalytic surface and favouring CO production along with H_2. Our results are consistent with those observed by Ramirez-Cabrera et al. when they compared their results on CGO to Ni/CGO catalysts for steam reforming of methane [15,16]. They concluded that Ni strongly increased the reforming rate and it also increased the risk of carbon deposition. The formation of carbon whiskers on Ni-based catalysts is well known and discussed in the literature. It is widely admitted that methane cracking operates through a successive C–H bond cleavage process. These carbon species may either condensate into non-reactive species (graphitic) or be oxidized to form CO. Depending on the relative kinetics of these two types of reactions carbon may accumulate on the catalyst or be removed. In the case of Ni catalysts, reactions leading to non-reactive carbon are kinetically favoured, irrespective of the support. It might be proposed that Ir, like Ni, easily activates CH_4 through CH_4 cracking (reaction (6)) to form reactive carbon species which readily react with highly reducible species of CGO support ($Ce^{4+} \to Ce^{3+}$). In addition, the nature of the carbon formed on Ir is different from carbon formed on Ni as further discussed.

Ir (0.1 wt%)/CGO tested in a large excess of methane shows a lower activity as compared to 7 wt%Ni/MgO catalyst developed by Wei et al. and tested in a stream containing much higher concentration of steam ($P_{CH_4} = 33.3$ kPa; $P_{H_2O} = 33.3$ kPa) [17] (Table 1). However the rates of methane consumption expressed per metal atom are surprisingly very close. On the other hand, it should be reminded that our aim is not to reach the best catalytic activity in H_2 production but a catalytic activity consistent with a gradual internal steam reforming operation.

The existence of an intermediate step of CH_4 cracking on Ir sites (Ir/CGO) in the overall mechanism is supported by TPR-CH_4 results obtained after completion of Ce^{4+} ions reduction into Ce^{3+}. Indeed, whenever no more oxygen species were available from the support, carbon deposits started to form. The key point for this catalyst is its capability to develop a limited amount of carbon at its surface, on the contrary to Ni catalysts and Ir/Al_2O_3. Above 800 °C, methane cracking on Ir/Al_2O_3 leads to hydrogen production and continuous carbon accumulation on the catalyst on the contrary to Ir/CGO. This suggests that the nature of the carbon formed on Ir catalysts is different depending on the support used (CGO and Al_2O_3).

For Ir/CGO and Ir/Al_2O_3, our experiments show that carbon species formed from methane cracking react with surface species of the support, being hydroxyls for Al_2O_3 or reducible oxygen species for CGO. CO formation rates derived from CH_4-TPR experiments over these two catalysts are quite different, being much higher for Ir/CGO. This could be explained either by the different nature and reactivity of carbon formed and/or by the hydroxyls groups of Al_2O_3 being less reactive than reducible surface CGO species. This is consistent with literature data showing that metal catalysts are not very active for methane steam reforming when supported on inert oxides [18].

Over CGO, the absence of any carbon formation even in dry methane atmosphere suggests, as described in a related study, a different mechanism involving the direct reaction of CH_4 with CGO, which would be much slower than CH_4 activation at Ir sites on Ir/CGO [13].

Finally, an increased reducibility of CGO in interaction with Ir is not ruled out. Noble metals supported on ceria-based catalysts used in 3-way converters were shown to drastically improve the reduction extent of the ceria component in the presence of reductants [19].

In this work, the high synergetic effect between Ir and CGO is likely associated with: (i) a strong metal–support interaction effect (SMSI) inducing a massive spillover of oxygen-species from the CGO onto the Ir catalyst surface, (ii) the specific nature and reactivity of carbon formed by methane cracking when Ir is supported on CGO. Ir species on CGO could not allow a carbon formation mechanism leading to the extensive non-reactive carbon accumulation observed on Ir/Al_2O_3. In addition, these Ir species would act as portholes for oxygen spillover and reaction with CH_4. This is a point which is well known both in the SOFC and in the electrochemical promotion communities [20]. Further investigations on the nature of Ir species present in Ir/CGO are being addressed.

5. Conclusions

Adding Ir to Gd-doped ceria at traces levels (less than 0.1 wt%) leads to a material with catalytic properties in steam reforming of methane comparable to Ni catalysts. Under strongly water deficient conditions thermodynamically favourable to carbon deposits formation, carbon did not accumulate on the contrary to Ni catalysts and Ir/Al_2O_3. This would be due to the different nature of carbon formed. Moreover, a bifunctional mechanism involving methane cracking on Ir sites to form reactive carbon species and facile reaction of the latter species with reducible sites of CGO was suggested. Overall results obtained in the present work validate the potential use of Ir/CGO as an anode component for SOFCs operating under GIR conditions.

Acknowledgements

The authors wish to acknowledge the French Government (Agence Nationale de la Recherche, PAN-H programme) under project CIEL and the European Union under project BIOGASFUELCELL (Marie–Curie incoming international fellowship MIF-CT-2006-039613) for financial support.

References

[1] J. Sfeir, J. Van Herle, J.A. McEvoy, Proc. 3rd European Solid Oxide Fuel Cell Forum, 1998, p. 267.
[2] E.S. Putna, J. Stubenrauch, J.M. Vohs, R.J. Gorte, Langmuir 11 (1995) 4832.
[3] A. Atkinson, S. Barnett, R.J. Gorte, J.T.S. Irvine, A.J. McEvoy, M.B. Mogensen, S. Singhal ad, J. Vohs, Nat. Mater. 3 (2004) 17.
[4] S.C. Singhal, K. Kendall, High Temperature Solid Oxide Fuel Cells: Fundamentals, Design, and Applications, Elsevier, 2003.
[5] S. Mclntosh, R.J. Gorte, Chem. Rev. 104 (2004) 4845.
[6] S.P. Jiang, S.H. Chan, J. Mater. Sci. 39 (2004) 4405.
[7] M. Mogensen, K. Kammer, Annu. Rev. Mater. Res. 33 (2003) 321.
[8] J.W. Fergus, Solid State Ionics 177 (2006) 1529.
[9] P. Vernoux, J. Guindet, M. Kleitz, J. Electrochem. Soc. 145 (1998) 3487.
[10] E. Perry Murray, T. Tsai, S.A. Barnett, Nature 400 (1999) 649.
[11] O.A. Marina, M. Mogensen, Appl. Catal. A: Gen. 189 (1999) 117.
[12] M. Wisniewski, A. Boréave, P. Gélin, Catal. Commun. 6 (2005) 596.
[13] B. Mosqueda, J. Toyir, A. Kaddouri, P. Gélin, Appl. Catal. B: Environ. 88 (2009) 361.
[14] G. Jacobs, U.M. Graham, E. Chenu, P.M. Patterson, A. Dozier, B.A. Davis, J. Catal. 229 (2005) 499.
[15] E. Ramirez-Cabrera, A. Atkinson, D. Chadwik, Appl. Catal. B: Environ. 47 (2004) 127.
[16] E. Ramirez-Cabrera, A. Atkinson, D. Chadwik, Appl. Catal. B: Environ. 36 (2002) 193.
[17] J. Wei, E. Iglesia, J. Catal. 224 (2004) 370.
[18] X. Wang, R.J. Gorte, Appl. Catal. A: Gen. 224 (2002) 209.
[19] A. Trovarelli, Catal. Rev.: Sci. Eng. 38 (4) (1996) 439–520.
[20] C.G. Vayenas, C.G. Koutsodontis, J. Chem. Phys. 128 (2008) 182506.